DALTON
FULL PAPER

Polynuclear molybdenum and tungsten complexes of 3-hydroxypicolinic acid and the crystal structures of $(^nBu_4N)_2[Mo_4O_{12}(picOH)_2]$ and $(^nHex_4N)_2[Mo_2O_6(picOH)_2]$

Susana M. O. Quintal,[a] Helena I. S. Nogueira,*[a] Helena M. Carapuça,[a] Vitor Félix[a] and Michael G. B. Drew[b]

[a] *Department of Chemistry, University of Aveiro, 3810-193 Aveiro, Portugal.*
E-mail: helena@dq.ua.pt
[b] *Department of Chemistry, The University, Whiteknights, Reading, UK RG6 6AD*

Received 17th April 2001, Accepted 14th August 2001
First published as an Advance Article on the web 11th October 2001

New polynuclear molybdenum(VI) and tungsten(VI) complexes with 3-hydroxypicolinic acid (HpicOH) $(^nBu_4N)_2[Mo_4O_{12}(picOH)_2]$ **1**, $(^nHex_4N)_2[Mo_2O_6(picOH)_2]$ **2**, $(BezPh_3P)_2[W_2O_6(picOH)_2]$ **3** (Bez = benzyl) and $[M_2O_5(picOH)_2]\cdot nH_2O$ (M = Mo(VI), *n* = 2 **4** or W(VI), *n* = 8 **5**) have been prepared. The crystal structures of **1** and **2** were determined by X-ray diffraction. The tetramolybdate **1** containing two coordinatively bound 3-hydroxypicolinate anions is a rare example of a discrete tetranuclear molybdenum-oxo cluster showing a Mo_4O_{12} core with the molybdenum centres bonded through oxo bridges only; the organic ligands being in a peripheral position. Infrared, ^1H and $^{13}C-\{^1H\}$ NMR spectroscopic data for the complexes are presented together with electrochemical characterization by cyclic voltammetry. These complexes are active toward oxygen atom transfer reactions and can catalyze the oxidation of benzoin (1,2-diphenyl-2-hydroxyethanone) with dmso.

Introduction

The current interest in derivatized polyoxometalates,[1] in particular those including organic components, is due to several aspects such as: structural analogues of polyoxometalates to metal oxide surfaces and their use as models for *e.g.* catalytic reactions at these type of surfaces; stabilization of otherwise unstable molecular architectures, providing novel building blocks for the assembly of larger systems; functionalization and selective recognition of substrates. In the case of polyoxomolybdates, the introduction of organic ligands has expanded their structural chemistry to include a variety of novel geometries constructed from corner-sharing and face-sharing of MoO_6 octahedra, in addition to the more common edge-sharing, and from tetrahedral[2] and square-pyramidal units, as well as the more common octahedral motifs.[3] Derivatized isopolymolybdate structures have been previously described, involving replacement of peripheral oxygen groups by other ligand units,[2,4] attachment of transition metal complexes,[5] or incorporation of organic groups into the heteropoly backbone.[2]

Here we report the synthesis and structure of a tetramolybdate $(^nBu_4N)_2[Mo_4O_{12}(picOH)_2]$ **1** containing coordinatively bound 3-hydroxypicolinate anion ($picOH^-$), and of a number of new binuclear molybdenum and tungsten complexes with $picOH^-$, $(^nHex_4N)_2[Mo_2O_6(picOH)_2]$ **2**, $(BezPh_3P)_2[W_2O_6(picOH)_2]$ **3**, $[Mo_2O_5(picOH)_2]\cdot 2H_2O$ **4** and $[W_2O_5(picOH)_2]\cdot 8H_2O$ **5**. The single crystal structures of **1** and **2** were determined. We have been studying[6] the coordination modes of $picOH^-$ in second and third row transition metal complexes. The molecular structures together with spectroscopic data for the molybdenum and tungsten complexes presented here, suggest that *N*,*O*-chelation of $picOH^-$ (coordination through the ring nitrogen and the carboxylate oxygen, forming a five-membered chelate ring) occurs in all complexes. *N*,*O*-chelation of $picOH^-$ has also been reported for vanadium,[7] rhenium,[6,8] ruthenium[9] and gold[10] complexes. In the case of palladium and platinum complexes,[6] coordination of $picOH^-$ is achieved primarily through the ring nitrogen but there is also a weak bonding interaction between the metal and the carboxylate oxygen, consistent with *N*,*O*-chelation.

Results and discussion

Preparations

Compound **1** was obtained by recrystallization in acetonitrile of the complex $(^nBu_4N)_2[Mo_2O_6(picOH)_2]$, which was prepared from an aqueous solution. The crystal structure of $[Mo_2O_6(picOH)_2]^{2-}$ was solved for the corresponding n-hexylammonium salt, compound **2**. The dimeric species $[M_2O_6(picOH)_2]^{2-}$ (M = Mo, compound **2**, or W, compound **3**) were obtained from an aqueous solution of MO_4^{2-} and the $picOH^-$ ligand; increasing the time of reaction gave rise to the $[M_2O_5(picOH)_2]$ species (M = Mo, compound **4**, or W, compound **5**), reflux temperature was needed for the molybdenum compound.

Crystal structures

The crystal structures of complexes $(^nBu_4N)_2[Mo_4O_{12}(picOH)_2]$ **1** and $(^nHex_4N)_2[Mo_2O_6(picOH)_2]$ **2** were determined by single crystal X-ray diffraction. Selected distances and angles in the molybdenum coordination sphere of these two complexes are given in Tables 1 and 2. The molecular structures of the complex anions $[Mo_4O_{12}(picOH)_2]^{2-}$ **1** and $[Mo_2O_6(picOH)_2]^{2-}$ **2** with the atomic numbering scheme used are shown in Fig. 1 and 2 respectively. The anions and their corresponding neutral species are labelled similarly.

As shown in Fig. 1, the tetramolybdate anion **1** consists of a Mo_4O_{12} core having the molybdenum centres linked through oxo bridges and two $picOH^-$ localized in peripheral positions, which are bonded to two molybdenum centres *via* *N*,*O*-chelation through the pyridine nitrogen donor and an oxygen atom from the adjacent carboxylate group. The structure has C_2 symmetry imposed by a two fold crystallographic axis perpendicular to the plane of the Mo_2O_2 central bridge.

DOI: 10.1039/b103348b

Table 1 Selected distances (Å) and angles (°) for complex **1**

Mo(1)–Mo(2)	3.219(3)	Mo(2)–O(1)	2.196(6)
Mo(1)–O(1)	2.086(5)	Mo(2)–O(2)	1.882(6)
Mo(1)–O(2)	1.940(5)	Mo(2)–O(5)	1.711(6)
Mo(1)–O(6)	1.677(7)	Mo(2)–O(4)	1.691(6)
Mo(1)–O(3)	1.691(6)	Mo(2)–O(22)	2.078(6)
Mo(1)–O(1*)	1.937(5)	Mo(2)–N(1)	2.373(7)
Mo(1*)–O(1)–Mo(1)	106.5(2)	Mo(1*)–O(1)–Mo(2)	152.4(3)
Mo(1)–O(1)–Mo(2)	97.4(2)	Mo(2)–O(2)–Mo(1)	114.7(3)
O(6)–Mo(1)–O(3)	108.2(4)	O(4)–Mo(2)–O(5)	104.8(3)
O(6)–Mo(1)–O(1*)	102.9(3)	O(4)–Mo(2)–O(2)	105.2(3)
O(3)–Mo(1)–O(1*)	97.7(3)	O(5)–Mo(2)–O(2)	101.1(3)
O(6)–Mo(1)–O(2)	102.9(3)	O(4)–Mo(2)–O(22)	92.1(3)
O(3)–Mo(1)–O(2)	96.2(3)	O(5)–Mo(2)–O(22)	97.2(3)
O(1*)–Mo(1)–O(2)	145.0(2)	O(2)–Mo(2)–O(22)	150.4(2)
O(6)–Mo(1)–O(1)	118.4(3)	O(4)–Mo(2)–O(1)	94.0(2)
O(3)–Mo(1)–O(1)	133.4(3)	O(5)–Mo(2)–O(1)	161.2(3)
O(1*)–Mo(1)–O(1)	73.0(2)	O(2)–Mo(2)–O(1)	72.7(2)
O(2)–Mo(1)–O(1)	74.1(2)	O(22)–Mo(2)–O(1)	82.5(2)
O(5)–Mo(2)–N(1)	85.4(3)	O(4)–Mo(2)–N(1)	162.2(3)
O(2)–Mo(2)–N(1)	86.6(2)	O(22)–Mo(2)–N(1)	71.9(2)
O(1)–Mo(2)–N(1)	76.6(2)		

* Denotes the symmetry operation x, $-y + 2$, $-z + 1$ used to generate equivalent atoms.

Table 2 Selected distances (Å) and angles (°) for complex **2**

Mo–Mo*	3.121(3)		
Mo–O(1)	2.184(4)	Mo–O(1*)	1.808(4)
Mo–O(2)	1.707(4)	Mo–O(3)	1.716(4)
Mo–O(22)	2.161(5)	Mo–N(1)	2.418(5)
Mo*–O(1)–Mo	102.4(1)		
O(3)–Mo–O(1)	160.6(2)	O(3)–Mo–O(1*)	103.0(2)
O(2)–Mo–O(1)	94.3(2)	O(2)–Mo–O(1*)	106.8(2)
O(2)–Mo–O(3)	103.9(2)	O(1*)–Mo–O(1)	77.6(1)
O(2)–Mo–O(22)	91.0(2)	O(3)–Mo–O(22)	92.8(2)
O(22)–Mo–O(1)	80.0(1)	O(1*)–Mo–O(22)	152.2(1)
O(1)–Mo–N(1)	78.0(2)	O(1*)–Mo–N(1)	88.7(2)
O(22)–Mo–N(1)	70.6(1)	O(3)–Mo–N(1)	82.5(2)
O(2)–Mo–N(1)	160.9(2)		

* Denotes the symmetry operation $-x + 1$, $-y$, $-z + 1$ used to generate equivalent atoms.

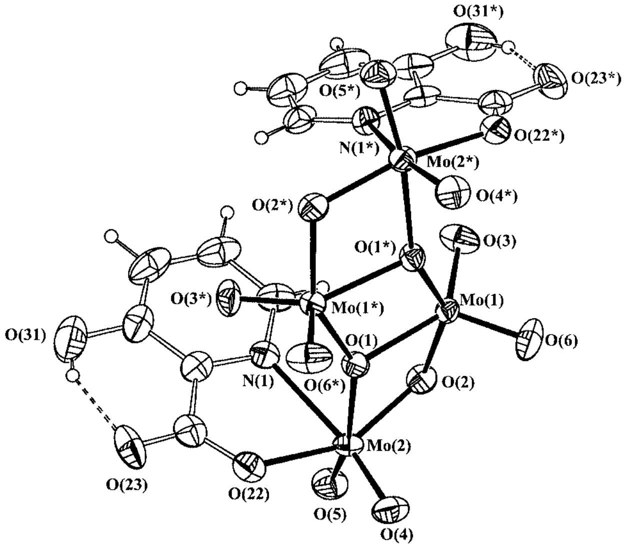

Fig. 1 An ORTEP[25] view of $[Mo_4O_{12}(picOH)_2]^{2-}$ **1** showing the atomic connectivities, labelling scheme adopted and thermal ellipsoids drawn at the 20% probability level.

In complex **1**, the two molybdenum centres Mo(1) of the Mo_2O_6 central sub core display a coordination geometry that can be described as a distorted square pyramid with an oxo group occupying an apical position. However, from the angles centred at these two metal centres, listed in Table 1, a significant distortion towards the bipyramidal geometry is apparent. The two terminal molybdenum centres Mo(2) display pseudo-octahedral coordination environments with the bond angles ranging between 71.9(2) and 161.2(3)° markedly deviated from the ideal angles for octahedral coordination. The oxo groups O(1) bridging the square pyramidal sites are also involved in the bridging to the octahedral sites and consequently these groups display a μ_3 coordination mode. In each of the molybdenum centres the two terminal oxo groups adopt the expected *cis*-configuration with O(6)–Mo(1)–O(3) and O(4)–Mo(2)–O(5) angles of 108.2(4) and 104.8(3)° respectively. Therefore, the structure of this tetramolybdate has a central binuclear core of two edge sharing $\{MoO_5\}$ square pyramids, each also sharing one edge with one of two peripheral $\{MoO_5N\}$ octahedra and one corner with the other.

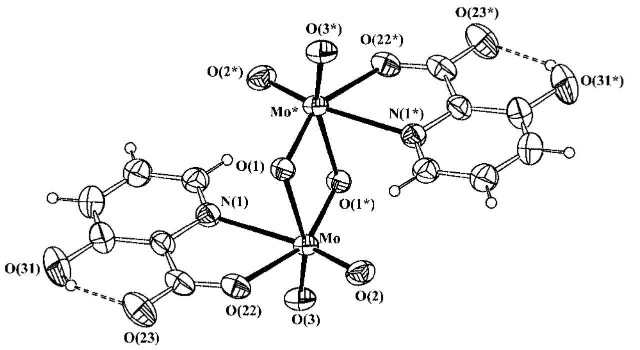

Fig. 2 An ORTEP view of $[Mo_2O_6(picOH)_2]^{2-}$ **2** showing the atomic connectivities, labelling scheme adopted and thermal ellipsoids drawn at the 20% probability level.

The structure of complex **1** is rare and to the best of our knowledge it is the first X-ray determination of a discrete tetranuclear molybdenum-oxo cluster showing a Mo_4O_{12} core with a ladder type structure. This ladder type structure is different from the usual cyclic Mo_4O_{12} core found in derivatized polyoxomolybdates,[1] in which the $[(MoO_2)_4(\mu\text{-}O)_4]$ core is stabilized by ligand bridges between the molybdenum centres. Indeed the structure of $[Mo_4O_{13}(Hbpa)_2]$ (Hbpa = 4-pyridyl-4′-pyridinium amine) is the only X-ray determination available from the Cambridge Structural Data Base[11] that contains similar polyhedral connectivity to that found for complex **1**. In the complex $[Mo_4O_{13}(Hbpa)_2]$, the sixth coordination site in the coordination sphere of the peripheral Mo(VI) is occupied by an oxo bridging group rather than by an oxygen donor from a carboxylate group as found for complex **1**. The former complex has a crystal structure composed of one-dimensional chains with $\{Mo_4O_{13}(Hbpa)_2\}$ units linked through two peripheral octahedra sharing a corner. On the other hand a search on the Inorganic Crystal Structure Database[12] located several structures of inorganic compounds having the fragment $[Mo_4O_{12}]$ but exhibiting markedly different molecular architectures. Thus, this observation suggests that the polyhedral connectivity of **1** and $[Mo_4O_{13}(Hbpa)_2]$ is stabilised by the presence of the organic ligands.

Although **1** and $[Mo_4O_{13}(Hbpa)_2]$ have identical polyhedral connectivities, a detailed analysis shows that these two structures have several different features, which should be emphasized. In complex **1** the two $picOH^-$ ligands are on the same side of the Mo_4 plane intersecting this plane at angles of 72.4(2)°. In contrast the complex $[Mo_4O_{13}(Hbpa)_2]$ has a centrosymmetric structure and consequently the two Hbpa ligands of the building block are on opposite sides of the Mo_4 plane adopting a perfectly anti-parallel configuration. Both complexes present a ladder (puckering) type structure as a consequence of the steric requirements of the edge and corner-sharing pattern of the molybdenum polyhedra. However, in complex **1** the {Mo(1),O(1)O(2),Mo(2)} and {Mo(1*),O(1*)O(2*),Mo(2*)} bridges intersect the {Mo(1),O(1)O(1*),Mo(1*)} bridge which links the two square pyramidal sites at an angle of 13.8(1)° which increases to 38.4° for $[Mo_4O_{13}(Hbpa)_2]$. Finally several bond distances and angles involving the molybdenum centres and oxo bridges are quite different in the two complexes leading to different intermolecular distances between the molybdenum centres. Thus in complex **1** the distance between the two square pyramidal sites is 3.224(3) Å while the square pyramidal sites are localized at 3.219(3) Å from the adjacent octahedral sites. These distances in $[Mo_4O_{13}(Hbpa)_2]$ are 3.321 and 3.406 Å respectively.

The binuclear complex $[Mo_2O_6(picOH)_2]^{2-}$ **2** shows a centrosymmetric structure composed by a $[Mo_2O_6]^0$ core bound to two $picOH^-$ ligands. Each of the molybdenum centres displays a pseudo-octahedral coordination sphere containing two bridging oxo groups and two terminal oxo groups. The six-coordination is completed with the pyridine nitrogen and an oxygen atom of the carboxylate from $picOH^-$ ligand, similar to that found in complex **1**. The two bridging oxo groups lie in the equatorial coordination plane and the structure can be described simply as two edge-sharing $MoO_4(picOH)$ octahedra. The two $picOH^-$ ligands are almost perpendicular to the plane of the Mo_2O_2 bridge intersecting at 85.0(2)°. Furthermore these ligands adopt a perfect anti-parallel configuration relative to the bridge plane. The Mo=O groups adopt the electronically favourable *cis* geometric arrangement with the O(1)–Mo–O(2) angle taking the value of 94.3(2)°. A search of the CSD[11] revealed many X-ray determinations of molybdate structures containing $[Mo_2O_6]^0$ cores stabilized in their molecular architectures, however, the presence of this core in binuclear dinegative species seems to be unusual and only five structures of this type are available. For example, $(^nBu_4N)_2[Mo_2O_6(C_5H_4NCO)_2]$ (C_5H_4NCO is 2-pyridine carboxylate) shows a structure with an overall geometry similar to that found for complex **2**. In fact the former complex also presents a centrosymmetric structure with the two 2-pyridine carboxylate ligands also bound to molybdenum *via N,O*-chelation and adopting an anti-parallel configuration as described for the studied complex **2**. Furthermore the two edge-sharing octahedral polyhedra have molecular comparable dimensions in both complexes. For example the intramolecular distance between the two molybdenum centres is 3.121(3) Å in **2** and 3.178(1) Å in $(^nBu_4N)_2[Mo_2O_6(C_5H_4NCO)_2]$.

As a consequence of the steric demands of the bite angle of the $picOH^-$ ligand the complexes described here present similar chelating angles of 71.9(2)° in **1** and 70.6(1)° in **2**. The Mo–N and $Mo–O_{carboxylate}$ distances in **1** are slightly shorter than those found in **2**.

The molecular assembly of $[Mo_4O_{12}(picOH)_2]^{2-}$ tetramolybdate anions and $^nBu_4N^+$ cations in **1** contains the $^nBu_4N^+$ cations aggregated in layers when the crystal structure is viewed perpendicularly to the [011] crystallographic plane, as shown in Fig. 3. The stacking of these layers results in the formation of large channels running through the crystal structure. The diameter of these channels is *ca.* 7.9 Å, which is the minimum distance between the hydrogen atoms of the cations across the cavities. Each of these channels composed of four chains of $^nBu_4N^+$ cations accommodates one chain of discrete $[Mo_4O_{12}(picOH)_2]^{2-}$ anions. The localization of the hydrogen atoms of cations on the walls of the channels suggests that the crystal structure is stabilized by hydrogen bonding interactions. In fact each of the anions is entrapped within the corresponding cavity through two short intermolecular $C–H^{\delta+}\cdots O^{\delta-}(=Mo)$ interactions involving two $H\cdots O$ distances of 2.385 Å with $C–H\cdots O$ angles of 155.1°. The molecular assembly of $[Mo_2O_6(picOH)_2]^{2-}$ and $^nHex_4N^+$ cations in **2** results in no special order in the crystal and no hydrogen bonding interactions were found between the two species.

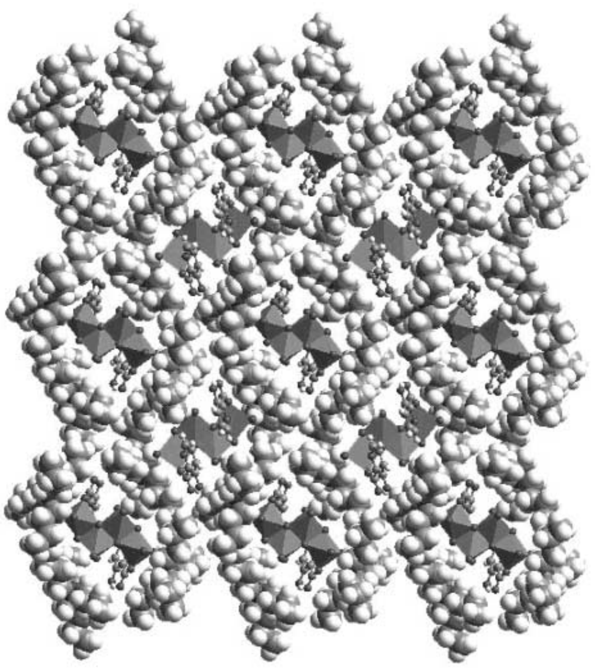

Fig. 3 Crystal packing diagram of $(^nBu_4N)_2[Mo_4O_{12}(picOH)_2]$ **1**. Viewed perpendicular to the [011] crystallographic plane, showing how the assembled $^nBu_4N^+$ cations define the channels which accommodate $[Mo_4O_{12}(picOH)_2]^{2-}$ anions. The anions are represented by showing the coordination polyhedra of the molybdenum centres while the $^nBu_4N^+$ cations are drawn in the ball mode.

Finally and as would be expected, hydrogen bonds between phenol and carbonyl groups of the $picOH^-$ ligands were found for both complexes **1** and **2** (see Fig. 1 and 2), but the atomic positions of the hydrogen atoms of the phenol group were calculated and consequently those hydrogen bonds are not analysed.

Vibrational spectra

Infrared spectroscopic data for 3-hydroxypicolinic acid (HpicOH) and its complexes are shown in Table 3, tentative assignments are based on those found in the literature for HpicOH complexes.[6] The selected bands of the free ligand, namely the carboxylate asymmetric and symmetric stretches, $\nu_{as}(CO_2)$ and $\nu_s(CO_2)$, and the C–O stretch of the hydroxyl group, $\nu(C–O)_h$, are sensitive to metal coordination as reported for complexes of hydroxybenzoic acids.[13,14] Shifts on coordination for the $\nu(C–O)_h$ stretch may be due to hydrogen bonding to the adjacent carboxylate group, as shown in the crystal structures of complexes **1** and **2**.

The symmetric metal *cis*-dioxo stretches, $\nu_s(MO_2)$ (M = Mo or W), are seen in the range 913–955 cm^{-1} as strong bands, with the asymmetric stretches, $\nu_{as}(MO_2)$, seen in the range 876–915 cm^{-1}. Very strong bands in the region 625–785 cm^{-1} may be assigned to the asymmetric metal oxo stretches, $\nu_{as}(M_2O)$ (M = Mo or W), of bridging oxo ligands;[2,15] medium intensity bands in the region 448–568 cm^{-1} may be assigned to the corresponding symmetric modes, $\nu_s(M_2O)$.[16]

The proposed formula for complexes **4** and **5** are based on elemental analysis and spectroscopic data, considering analogous complexes that have been reported for other bidentate ligands, such as $(NH_4)_2[Mo_2O_5(nd)_2)]\cdot 2H_2O$[16] ($H_2nd$ = naphthalene-2,3-diol).

^1H and ^{13}C-{^1H} NMR spectra

Proton and carbon NMR data and tentative assignments for HpicOH (see Chart 1 for labelling) and complexes are given in Table 4. In the ^{13}C NMR spectra the carboxylic carbon of the $picOH^-$ ligand, C_7, shows a downfield shift ranging from 6.5 to

Table 3 Analytical and spectroscopic data for complexes of 3-hydroxypicolinic acid and the free ligand

	Analysis[a] (%)			Infrared spectra/cm^{-1}						
Compound	C	H	N	$\nu_{as}(CO_2)$	$\nu_s(CO_2)$	$\nu(C–O)_h$	$\nu_s(MO_2)$	$\nu_{as}(MO_2)$	$\nu_{as}(M_2O)$	$\nu_s(M_2O)$
3-Hydroxypicolinic acid				1654 vs	1322 s	1283 s				
$(^{n}Bu_4N)_2[Mo_4O_{12}(picOH)_2]$ **1**	38.9 (39.5)	5.9 (6.0)	4.2 (4.2)	1654 s	1323 vs	1266 s	955 m, 945 s, 935 s	915vs, 904 s, 891 m	727 s, 688 vs	568 m
$(^{n}Hex_4N)_2[Mo_2O_6(picOH)_2]$ **2**	56.2 (56.6)	8.9 (8.9)	4.3 (4.4)	1645 vs	1332 s	1264 s	921 s, 913 s	876 vs, 890 s	749 vs	466 m
$(BezPh_3P)_2[W_2O_6(picOH)_2]$ **3**	50.1 (51.5)	3.7 (3.6)	2.2 (1.9)	1642 vs	1336 s	1257 s	938 s	892 vs	690 vs	512 s
$[Mo_2O_5(picOH)_2]·2H_2O$ **4**	24.7 (24.7)	2.3 (2.1)	4.7 (4.8)	1650 vs	1319 s	1244 vs	945 vs	901 vs	785 vs	460 s
$[W_2O_5(picOH)_2]·8H_2O$ **5**	16.6 (16.6)	2.6 (2.8)	2.9 (3.2)	1643 vs	1336 m	1259 s	934 vs	893 vs	625 vs	448 m

[a] Calculated values in parentheses.

Table 4 ^1H and $^{13}C-\{^1H\}$ NMR spectroscopic data for 3-hydroxypicolinic acid and its complexes[a]

	Chemical shift (δ)								
Compound	H_4	H_5	H_6	C_2	C_3	C_4	C_5	C_6	C_7
3-Hydroxypicolinic acid	7.96	7.86	8.19	134.4	161.1	130.8	130.9	134.2	166.8
$(^{n}Bu_4N)_2[Mo_4O_{12}(picOH)_2]$ **1**	7.58	7.65	8.65	142.5[b]	157.3[b]	129.9[b]	132.9[b]	137.4[b]	173.3[b]
$(^{n}Hex_4N)_2[Mo_2O_6(picOH)_2]$ **2**	7.58	7.65	8.67	141.1	159.7	128.9	130.3	133.3	173.5
$(BezPh_3P)_2[W_2O_6(picOH)_2]$ **3**	7.63	7.71	8.65	141.3	160.0	129.6	130.7	133.0	174.7
$[Mo_2O_5(picOH)_2]·2H_2O$ **4**	7.82	7.78	8.43	143.7	159.6	131.7	132.0	132.9	173.4
$[W_2O_5(picOH)_2]·8H_2O$ **5**	7.65	7.69	8.66	141.4	160.1	130.8	129.7	133.0	174.7

[a] Spectra in CD_3OD solution unless otherwise stated. [b] CPMAS solid state NMR data.

Table 5 Electrochemical data for the complexes[a]

Compound	E_{pc}/mV	E_{pa}/mV
$(^{n}Bu_4N)_2[Mo_4O_{12}(picOH)_2]$ **1**	−980	730[b]
$(^{n}Hex_4N)_2[Mo_2O_6(picOH)_2]$ **2**	−1530	643
$(BezPh_3P)_2[W_2O_6(picOH)_2]$ **3**	−2074	662
$[Mo_2O_5(picOH)_2]·2H_2O$ **4**	−945[c]	727[c]
$[W_2O_5(picOH)_2]·8H_2O$ **5**	−1345	620

[a] Potentials are recorded *versus* the Ag/Ag$^+$ reference electrode at room temperature, scan rate = 20 mV s^{-1} unless otherwise stated. [b] Scan rate = 100 mV s^{-1}. [c] Scan rate = 50 mV s^{-1}.

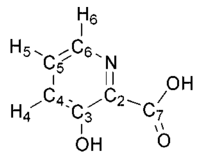

Chart 1

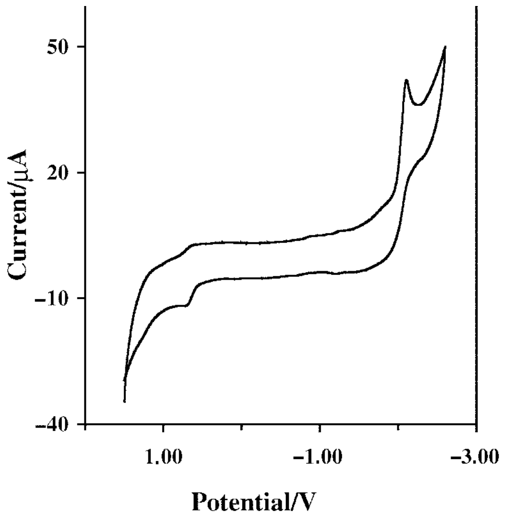

Fig. 4 Cyclic voltammogram of $(BezPh_3P)_2[W_2O_6(picOH)_2]$ **3** in CH_3CN containing 0.2 mol dm^{-3} $[Bu_4N][PF_6]$ (scan rate = 20 mV s^{-1}).

7.9 ppm, for all complexes. This shift supports a carboxyl group bonded to a high-valent metal.[14] There is also a considerable downfield shift in C_2 ranging from 6.7 to 9.3 ppm, shown in the spectra of all complexes. The significant shifts in the resonances of C_7 and C_2 together with the fact that the position of the phenolic carbon atom C_3 is little altered, is consistent[6] with *N*,*O*-chelation in all complexes (shown in the crystal structures of **1** and **2**).

Electrochemistry

The electrochemical behaviour of the complexes was studied by cyclic voltammetry at the glassy carbon electrode and in a solution of electrolyte, $[Bu_4N][PF_6]$ 0.2 M, in CH_3CN for complexes **2** and **3**, and in dmf for complexes **1**, **4** and **5**. Ferrocene was added in all measurements as an internal reference. Electrochemical data for the complexes are given in Table 5. All complexes show an irreversible voltammetric response associated with the metal centre at the glassy carbon electrode, in the potential range −980 to −2074 mV (*versus* the Ag/Ag$^+$ reference electrode). The voltammogram of $(BezPh_3P)_2[W_2O_6(picOH)_2]$ **3** is given in Fig. 4 as a representative example. This irreversible reduction is typical of MoO_2[17] and WO_2[18] units and this response can be assigned to the one electron transfer per molybdenum or tungsten comprising the M(VI)-dioxo and M(V)-oxo complexes. The potential of complex **5** is more negative than that of complex **4**, as expected for the reduction of the W(VI) metal center. These results are consistent with reported studies of Mo(VI) and similar W(VI) complexes.[19,20] Apparently, there are no reversible systems present. In the positive potential region the complexes display one oxidation peak between 620 and 730 mV assignable to the oxidation of the ligand. Interestingly, there is a dependence of the metal reduction peak potential on the counter-ion. In fact, for complexes **1**, **2** and **3**, the potential of the reduction peak, E_{pc}, becomes more negative as the size of the counter-ion increases (for complex **3** there is also the effect of having a W(VI) metal centre). This might be due to steric hindrance effects.

Table 6 Percentage conversion of benzoin into benzil after 6 and 24 hours[a]

Catalyst	Conversion (%) 6 h	Conversion (%) 24 h
$(^{n}Bu_4N)_2[Mo_4O_{12}(picOH)_2]$ **1**	48	99
$(^{n}Hex_4N)_2[Mo_2O_6(picOH)_2]$ **2**	61	99
$(BezPh_3P)_2[W_2O_6(picOH)_2]$ **3**	12	13
$[Mo_2O_5(picOH)_2]\cdot 2H_2O$ **4**	15	25
$[W_2O_5(picOH)_2]\cdot 8H_2O$ **5**	5	6

[a] Metal complexes were treated with 25 equivalents of benzoin in deoxygenated CD_3SOCD_3 at 100 °C.

Oxo-transfer properties

The oxo-transfer properties of the molybdenum and tungsten complexes were studied using a standard reaction[20] with benzoin as the reductant and dimethylsulfoxide (dmso) as the oxo donor. All complexes are able to catalyse the oxidation of benzoin to benzil (1,2-diphenylethan-1,2-dione) by dmso. However, the ([benzoin]+[benzil])/[catalyst] ratios increase gradually during the course of the reactions, indicating that part of the catalyst is deactivated and consumed. Table 6 shows the percentage conversion of benzoin into the oxidation product after 6 and 24 h. After 24 hours the conversion of benzoin to benzil was about 100% for complexes **1** and **2**. For complex **4** there was 25% conversion after 24 h. For the tungsten complexes the percentage of benzoin to benzil conversion is smaller than for the molybdenum complexes and there is no significant change from 6 to 24 h of reaction. The higher reactivity of the molybdenum complexes as catalysts in the oxo-transfer reactions relative to the tungsten complexes can be explained by their less negative reduction potentials and the weaker Mo=O bond.[20]

Experimental

Preparation of complexes

All chemicals were of at least reagent grade and used as supplied by Aldrich.

Instrumentation

Infrared spectra were measured as KBr pellets on a Mattson 7000 FT instrument. ^1H and ^{13}C NMR spectra were recorded on a Brüker AMX300 spectrometer (^1H, 300 MHz; ^{13}C, 75.4 MHz) referenced to $SiMe_4$ or the solvent. CPMAS ^{13}C NMR spectra were recorded on a Brüker MSL 400P spectrometer at 100.6 MHz with a 4.5 μs 90° pulse and a contact time of 2 ms. Electrochemical measurements were carried out with a BAS 100W electrochemical analyser, with a conventional three electrode system cell. A glassy carbon disc (diameter 3 mm) was used as the working electrode, a platinum wire as the counter electrode and the reference electrode was $Ag–AgNO_3$, 0.01 M in 0.2 M $Bu_4NPF_6–CH_3CN$ (Ag/Ag^+ reference electrode). The electrolyte was 0.2 M Bu_4NPF_6 in CH_3CN or in dmf. Cyclic voltammetry was carried out at room temperature, in 1 mM sample solutions. All solutions were purged with nitrogen before measurements. Ferrocene was added as an internal reference for the calibration of the Ag/Ag^+ reference electrode (0.086 V *vs.* Fc). All potentials quoted are relative to the Ag/Ag^+ reference electrode. Microanalyses (C, H and N) were measured by the Department of Chemistry, University of Aveiro.

Syntheses

$(^{n}Bu_4N)_2[Mo_4O_{12}(picOH)_2]$ (1). 3-Hydroxypicolinic acid (0.28 g, 2 mmol) was added to an aqueous solution (10 cm^3) of $Na_2MoO_4\cdot 2H_2O$ (0.24 g, 1 mmol) to give a beige solution. An aqueous solution (5 cm^3) of tetrabutylammonium chloride (0.56 g, 2 mmol) was added. The resulting solution was stirred for 30 minutes and centrifuged. A beige solid was isolated, washed with water and dried over silica gel. Yield of beige solid: 0.174 g (32%). Anal. of beige solid, for $(^{n}Bu_4N)_2[Mo_2O_6(picOH)_2]$, $C_{44}H_{80}Mo_2N_4O_{12}$. Calc.: C, 50.4; H, 7.7; N, 5.3. Found: C, 50.5; H, 7.7; N, 5.2%. Compound **1** was obtained, as beige X-ray quality crystals, by recrystallization of the beige solid in acetonitrile.

$(^{n}Hex_4N)_2[Mo_2O_6(picOH)_2]$ (2). 3-Hydroxypicolinic acid (0.278 g, 2 mmol) was added to an aqueous solution (5 cm^3) of $Na_2MoO_4\cdot 2H_2O$ (0.24 g, 1 mmol) to give a beige solution. An aqueous solution (20 cm^3) of tetrahexylammonium chloride (0.78 g, 2 mmol) was added. The resulting beige suspension was centrifuged. A beige solid was isolated, washed with water and dried over silica gel. Yield: 0.364 g, 0.286 mmol, 57%. Beige X-ray quality crystals of $(^{n}Hex_4N)_2[Mo_2O_6(picOH)_2]$ were obtained from the centrifuged solution after a few days.

$(BezPh_3P)_2[W_2O_6(picOH)_2]$ (3). 3-Hydroxypicolinic acid (0.278 g, 2 mmol) was added to an aqueous solution (5 cm^3) of $Na_2WO_4\cdot 2H_2O$ (0.33 g, 1 mmol) to give a beige suspension. An aqueous solution (20 cm^3) of benzyltriphenylphosphonium chloride (0.78 g, 2 mmol) was added. The beige solid was isolated, washed with water and dried over silica gel. Yield: 0.62 g, 0.429 mmol, 86%.

$[Mo_2O_5(picOH)_2]\cdot 2H_2O$ (4). 3-Hydroxypicolinic acid (0.33 g, 2.5 mmol) was added to an aqueous solution (20 cm^3) of $Na_2MoO_4\cdot 2H_2O$ (0.24 g, 1 mmol) to give a beige solution. An aqueous solution (5 cm^3) of tetraethylammonium chloride (0.28 g, 2 mmol) was added. The resulting solution was stirred for 15 minutes and then refluxed for 7 hours. Most of the solvent was evaporated and a beige solid was isolated, washed with water and ethanol and dried over silica gel. Yield: 0.182 g, 0.323 mmol, 65%.

$[W_2O_5(picOH)_2]\cdot 8H_2O$ (5). 3-Hydroxypicolinic acid (0.278 g, 2 mmol) was added to an aqueous solution (10 cm^3) of $Na_2WO_4\cdot 2H_2O$ (0.33 g, 1 mmol) to give a beige suspension. The beige suspension was stirred overnight and then centrifuged. A white solid was isolated, washed with water and dried over silica gel. Yield: 0.15 g, 0.173 mmol, 35%.

Oxo-transfer reactions

The reactions were carried out using the method of Wong *et al.*[20] In general, 0.01 mmol of the complexes **1** to **5** and 25 equivalents of benzoin were dissolved in deoxygenated CD_3SOCD_3 (0.5 cm^3). The mixtures were sealed in NMR tubes under nitrogen and heated at 100 °C. The reactions were monitored by ^1H NMR spectroscopy, which allowed the quantification of benzoin and benzil as well as the metal complexes.

Crystallography

Table 7 summarizes the crystal data together with refinement details for complexes **1** and **2**.

The X-ray data for these two complexes were collected on a MAR research plate system using graphite Mo-Kα radiation at Reading University. The crystals were positioned 70 mm from the image plate. 95 frames were measured at 2° intervals using a counting time between 2 and 10 min appropriate to the crystal under study. Data analysis was carried out with the XDS program.[21] Intensities of *hkl* data were not corrected for absorption effects. The structures were solved by a combination of direct methods, Fourier-difference syntheses and subsequent full-matrix least-squares refinements on F^2. All hydrogen atoms,

Table 7 Room temperature crystal data and the pertinent refinement parameters for complexes **1** and **2**

	1	**2**
Formula	$C_{44}H_{80}Mo_4N_4O_{18}$	$C_{60}H_{112}Mo_2N_4O_{12}$
M	1336.88	1273.42
Crystal system	Orthorhombic	Monoclinic
Space group	$P22_12_1$	$P2_1/n$
T/K	293(2)	293(2)
a/Å	8.758(11)	15.233(21)
b/Å	17.540(23)	15.273(23)
c/Å	18.560(25)	16.196(27)
β/°	(90.0)	115.70(1)
V/Å^3	2851(6)	3395(9)
Z	2	2
D_c/g cm^{-3}	1.557	1.246
μ/mm^{-1}	0.927	0.426
F(000)	1368	1360
Reflections measured	8475	6003
Unique reflections	4826 (R_{int} = 0.0236)	6003(R_{int} = 0.000)
Final R indices [$I > 2\sigma(I)$] R_1 and wR_2	0.0481, 0.1140	0.0546, 0.1416
R indices (all data) R_1 and wR_2	0.0748, 0.1291	0.0912, 0.1634

including the hydrogen of the phenol group, were introduced in the refinement at the geometric idealized positions giving isotropic thermal parameters equal to 1.2 times that of the parent atom.

All calculations required to solve and refine the structures were carried out with SHELXS and SHELXL from the SHELX-97 package.[22] Molecular diagrams were drawn with CERIUS2[23] and PLATON[24] graphical interfaces.

CCDC reference numbers 162915 and 162916.

See http://www.rsc.org/suppdata/dt/b1/b103348b/ for crystallographic data in CIF or other electronic format.

Acknowledgements

The authors would like to acknowledge Fundação para a Ciência e a Tecnologia (FCT) for financial support. S. M. O. Quintal thanks the FCT for a postgraduate grant. We also thank the EPSRC (UK) and the University of Reading (UK) for funds for the Image Plate System and Mr A. W. Johans for his assistance with the crystallography.

References

1 P. Gouzerh and A. Proust, *Chem. Rev.*, 1998, **98**, 77.
2 T.-C. Hsieh and J. A. Zubieta, *Polyhedron*, 1986, **5**, 305.
3 J. Zubieta, in *Polyoxometalates: From Platonic Solids to Anti-Retroviral Activity*, ed. M. T. Pope and A. Müller, Kluwer, Dordrecht, 1994, p. 129.
4 H. Kwen, V. G. Young, Jr. and E. A. Maatta, *Angew. Chem., Int. Ed.*, 1999, **38**, 1145.
5 J. Q. Xu, R. Z. Wang, G. Y. Yang, Y. H. Xing, D. M. Li, W. M. Bu, L. Ye, Y. G. Fan, G. D. Yang, Y. Xing, Y. H. Lin and H. Q. Jia, *Chem. Commun.*, 1999, 983.
6 S. M. O. Quintal, H. I. S. Nogueira, V. Félix and M. G. B. Drew, *New J. Chem.*, 2000, **24**, 511.
7 A. Shaver, J. B. Ng, D. A. Hall, B. S. Lum and B. I. Posner, *Inorg. Chem.*, 1993, **32**, 3109.
8 S. Gatto, T. I. A. Gerber, G. Bandoli, J. Perils and J. G. H. Preez, *Inorg. Chim. Acta*, 1998, **269**, 235.
9 V. L. Constantino, L. C. Oliveira, P. S. Santos and H. Toma, *Transition Met. Chem.*, 1994, **19**, 103.
10 A. Dar, K. Moss, S. M. Cottrill, R. V. Parish, C. A. McAuliffe, R. G. Pritchard, B. Beagley and J. Sandbank, *J. Chem. Soc., Dalton Trans.*, 1992, 1907.
11 F. H. Allen, J. E. Davies, J. J. Galloy, O. Johnson, O. Kennard, C. F. Macrae, E. M. Mitchell, G. F. Mitchel, J. M. Smith and D. G. Watson, *J. Chem. Inf. Comp. Sci.*, 1991, **31**, 187; P. J. Zapf, R. L. LaDuca, Jr., R. S. Rarig, Jr., K. M. Johnson III and J. Zubieta, *Inorg. Chem.*, 1998, **37**, 3411.
12 G. Bergerhoff, R. Hundt, R. Sievers and I. D. Brown, *J. Chem. Inf. Comp. Sci.*, 1983, **23**, 66.
13 W. P. Griffith, H. I. S. Nogueira, B. C. Parkin, R. N. Sheppard, A. J. P. White and D. J. Williams, *J. Chem. Soc., Dalton Trans.*, 1995, 1775.
14 C. F. Edwards, W. P. Griffith, A. J. P. White and D. J. Williams, *J. Chem. Soc., Dalton Trans.*, 1993, 3813.
15 A. Lehtonen and R. Sillanpää, *J. Chem. Soc., Dalton Trans.*, 1994, 2119.
16 A. M. El-Hendawy, W. P. Griffith, C. A. O'Mahoney and D. J. Williams, *Polyhedron*, 1989, **8**, 519.
17 J. M. Berg and R. H. Holm, *J. Am. Chem. Soc.*, 1985, **107**, 917; M. Chaudhury, *J. Chem. Soc., Dalton Trans.*, 1984, 115; N. Ueyama, H. Oku, M. Kondo, T. Okamura, N. Yoshinaga and A. Nakamura, *Inorg. Chem.*, 1996, **35**, 643.
18 M. R. Maurya, D. C. Antony, S. Gopinathan, V. G. Puranik, S. S. Tavale and C. Gopinathan, *Bull. Chem. Soc. Jpn.*, 1995, **68**, 2847; C. A. Rice, P. M. H. Kroneck and M. T. Spence, *Inorg. Chem.*, 1981, **20**, 1996.
19 Y. L. Wong, J. F. Ma, W. F. Law, W. T. Wong, Z. Y. Zhang, T. C. W. Mak and D. K. P. Ng, *Eur. J. Inorg. Chem.*, 1999, 313; C. A. Rice, P. M. H. Kroneck and M. T. Spence, *Inorg. Chem.*, 1981, **20**, 1996.
20 Y. L. Wong, Y. Yan, E. S. H. Chan, Q. Yang, T. C. W. Mak and D. K. P. Ng, *J. Chem. Soc., Dalton Trans.*, 1998, 3057.
21 W. Kabsch, *J. Appl. Crystallogr.*, 1988, **21**, 916.
22 G. M. Sheldrick, SHELX-97, University of Göttingen, Germany, 1997.
23 CERIUS2, version 3.5, Molecular Simulations Inc., San Diego, 1997.
24 A. L. Spek, PLATON, A Multipurpose Crystallographic Tool, Utrecht University, Utrecht, The Netherlands, 1999.
25 C. K. Johnson, ORTEP, Report ORNL-5138, Oak Ridge National Laboratory, Oak Ridge, TN, 1976.